Low frequency EPR of *Pseudomonas aeruginosa* azurin

Analysis of ligand superhyperfine structure from a type 1 copper site

William E. Antholine,* Phillip M. Hanna,‡ and David R. McMillin‡

*National Biomedical ESR Center, Biophysics Research Institute, Medical College of Wisconsin, Milwaukee, Wisconsin 53226 USA; and
‡Department of Chemistry, Purdue University, West Lafayette, Indiana 47907 USA

ABSTRACT The type 1 copper in *Pseudomonas aeruginosa* azurin was studied by electron paramagnetic resonance (EPR) spectroscopy at low microwave frequencies. Partially resolved ligand hyperfine structure was observed in the perpendicular region of the spectra at both S-band (2.4 GHz) and L-band (1.1 GHz). A trial and error method, requiring several hundred simulations, has been used to simulate the low frequency EPR data and yield an optimum value of 30 MHz for A_x^{Cu}, more than one half that previously reported. The fit between the simulated and experimental data is sensitive to changes in the Euler angles and, in particular, to the angle α which rotates the Cu *A*-tensor about the *z*-axis. Thus, the *A*- and *g*-tensors for copper in *P. aeruginosa* azurin do not appear to be coincident. A value for the Euler angle β of at least 10° does not disturb the fit between the simulated and experimental data. These studies demonstrate the advantage of evaluating EPR parameters from simulations at more than one frequency, especially at low frequencies where ligand superhyperfine structure may be resolved for type 1 copper.

INTRODUCTION

The azurins are blue copper proteins which are invariably involved in bacterial electron transfer processes. They belong to a group of blue copper proteins called cupredoxins, which bind only type 1 copper (1). This single-domain protein from *Pseudomonas aeruginosa* binds one copper ion per molecule at a binding site ~7 Å from the protein surface (2). The binding geometry about the copper is known in detail from the x-ray crystal structure, and consists of a distorted trigonal bipyramidal conformation (2, 3). Two histidine residues (His46 N^{δ} and His117 N^{δ}) and a cysteine residue (Cys112 S^{γ}) are coordinated somewhat equatorially 2.0–2.2 Å from the copper, with a methionine sulfur (Met121 S^{δ}) and a carbonyl oxygen (Gly45 O) occupying the more distant axial positions at 3.0–3.1 Å (2). The binding site in *Alcaligenes denitrificans* azurin is very similar to that found in *P. aeruginosa* azurin (4).

Two characteristics readily distinguish type 1 copper from copper bound in other environments. The first is an intense Cys-S-to-copper charge-transfer absorption at ~600 nm, which give proteins with type 1 copper their characteristic blue color (5, 6). The other distinguishing characteristic is its electron paramagnetic resonance (EPR) spectrum, where the hyperfine coupling constant along the symmetry axis ($g_{||}$) for type 1 Cu(II) is approximately half (150–270 MHz) of that typically observed for simple Cu(II) complexes (7). The type 1 Cu(II) EPR spectra for azurin and blue copper proteins in general have been studied extensively at J-, X-, and Q-bands at 6, 9, and 35 GHz, respectively (8, 9). Electron-nuclear double resonance (ENDOR) spectroscopy at these frequencies has also revealed details of the electronic structure at the copper site from analysis of the ligand hyperfine couplings (10, 11).

Because the linewidths of EPR transitions are affected by a distribution of magnetic parameters (i.e., strain), the best resolution of the hyperfine and superhyperfine structures occur at lower microwave frequencies for simple Cu(II) complexes (12). The number of nitrogen donor atoms to Cu(II) in a variety of complexes can be determined from the superhyperfine or ligand hyperfine pattern resolved on one of the Cu hyperfine lines (typically the $M_I = -1/2$ transition at 2–3 GHz) in the $g_{||}$ region of the spectrum (e.g., see reference 13 and references within). EPR spectra of metal ions bound at protein sites are typically prone to more broadening from strain than those of simple Cu(II) complexes (9). However, ligand hyperfine resolved only in the $g_{\perp}$ region at X-band, has been resolved in both the $g_{\perp}$ and $g_{||}$ regions at S-band (2.4 GHz) for the type 1 copper in *Polyporus versicolor* laccase, a multicopper oxidase (14).

In this study, we have examined the low frequency EPR spectra of the type 1 copper site in *Pseudomonas aeruginosa* azurin at S- and L-bands (2.3–2.4 GHz and 1.1–1.2 GHz, respectively). At these frequencies, ligand superhyperfine structure is resolved in the $g_{\perp}$ region but not in the $g_{||}$ region of the spectra. Simulations of this newly resolved fine structure at low frequencies are used to evaluate the parameters previously determined from EPR and ENDOR experiments at X-band and Q-band. The advantage of a multifrequency approach is described, where the resolved superhyperfine structure becomes a sensitive reporter for obtaining refined EPR parameters from simulations.

MATERIALS AND METHODS

Preparation of azurin samples

Azurin was isolated from a bacterial cultivation of *P. aeruginosa* (strain No. 10145; American Type Culture Collection) according to

P. M. Hanna's present address is Laboratory of Molecular Biophysics, National Institute of Environmental Health Sciences, National Institutes of Health, P.O. Box 12233, Research Triangle Park, North Carolina 27709.

0006-3495/93/01/267/06 $2.00

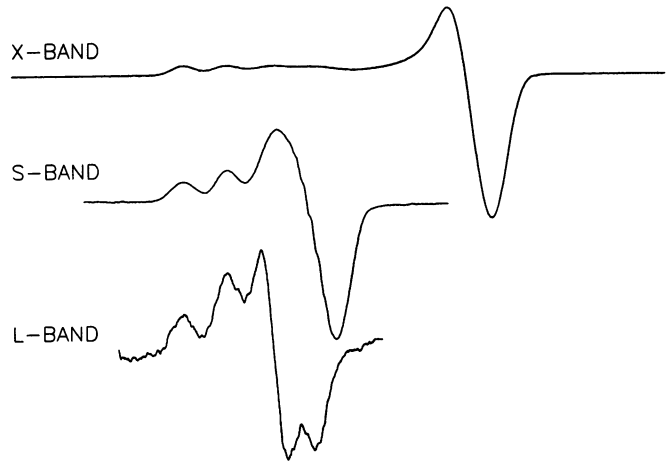

FIGURE 1 Multifrequency EPR spectra of the cupric site of azurin. Spectrometer conditions: X-band (9.13 GHz), 7.4 K; S-band (2.38 GHz), 120 K; L-band (1.14 GHz), 120 K; modulation amplitude, 5 G; modulation frequency, 100 kHz.

the method of Ambler and Brown (15). Protein purity was determined by monitoring the ultraviolet absorption below 280 nm as well as the ratio of the absorbance maxima at 624 and 280 nm. Azurin with an absorbance ratio of ~0.46 was used for this work. Recent work, however, suggests the presence of non-metalated protein for preparations with an absorbance ratio < 0.5 (16), but this is not expected to affect the EPR results.

Isotopically pure ^{65}Cu(II)-azurin was prepared by first preparing the apoprotein by anaerobic dialysis against 0.1 M thiourea, 0.25 M NaCl, and 5 mM sodium ascorbate in 50 mM pH 4 ammonium acetate (16). Immediately following removal of the thiourea by dialysis against 25 mM pH 8 tris buffer (Sigma Chemical Co., St. Louis, Missouri), the apoazurin was incubated with a 1.5-fold excess of ^{65}Cu(II) (prepared by dissolution of isotopically enriched CuO from Oakridge Laboratory in a minimal amount of HCl). The reconstituted azurin was purified by dialysis against 0.1 M pH 6 sodium phosphate for analysis. The protein was kept at 4°C at all times during sample preparation.

EPR experiments

EPR spectra at X-band (9.16 GHz) were recorded on a Varian Century Series spectrometer (Palo Alto, California). A Gauss meter (MH-110R Radiopan, NMR magnetometer) was used to calibrate the magnetic field and a frequency counter (EIP model 548) was used to determine the microwave frequency. Loop-gap resonators and low frequency bridges used for measurement at S- (2.4 GHz) and L-band (1.1 GHz) frequencies were designed and built at the National Biomedical ESR Center (12, 18). Temperatures were maintained with an Air Products (Allentown, Pennsylvania) helium flow system. The first harmonic of first derivative spectra were obtained using SUMSPEC92, a data manipulation program available upon request from the National Biomedical ESR Center in Milwaukee (19).

Simulations

EPR spectra were simulated with the QPOW program (20, 21) obtained from the Illinois Electron Spin Resonance Center, Urbana, Illinois (National Institutes of Health, National Center for Research Resources). Matrix diagonalization of the Zeeman and hyperfine terms are coupled with perturbation treatment of the superhyperfine interactions. The spin Hamiltonian for QPOW has the following terms: $\mathcal{H} = \beta H \cdot g \cdot \mathbf{S} + \mathbf{I} \cdot A \cdot \mathbf{S} + g_N \beta_N H \cdot \mathbf{I} + \mathbf{I} \cdot P \cdot \mathbf{I}$, where β is the Bohr magneton; β_N, the nuclear magneton; H, the magnetic field; A, the hyperfine tensor; S and I, the vectors for electron and nuclear spin. In this study, Gaussian lineshapes were employed.

RESULTS AND DISCUSSION

Multifrequency EPR spectra of the type 1 copper site of azurin

First derivative EPR spectra for ^{65}Cu-azurin at X-, S- and L-bands are shown in Fig. 1. Ligand superhyperfine structure was not resolved at X-band, even at 7.4 K (Fig. 1). At 123 K, however, ligand superhyperfine structure was clearly visible in the perpendicular region of the spectrum at S-band (Fig. 1). The resolution of this superhyperfine structure was enhanced in the second deriv-

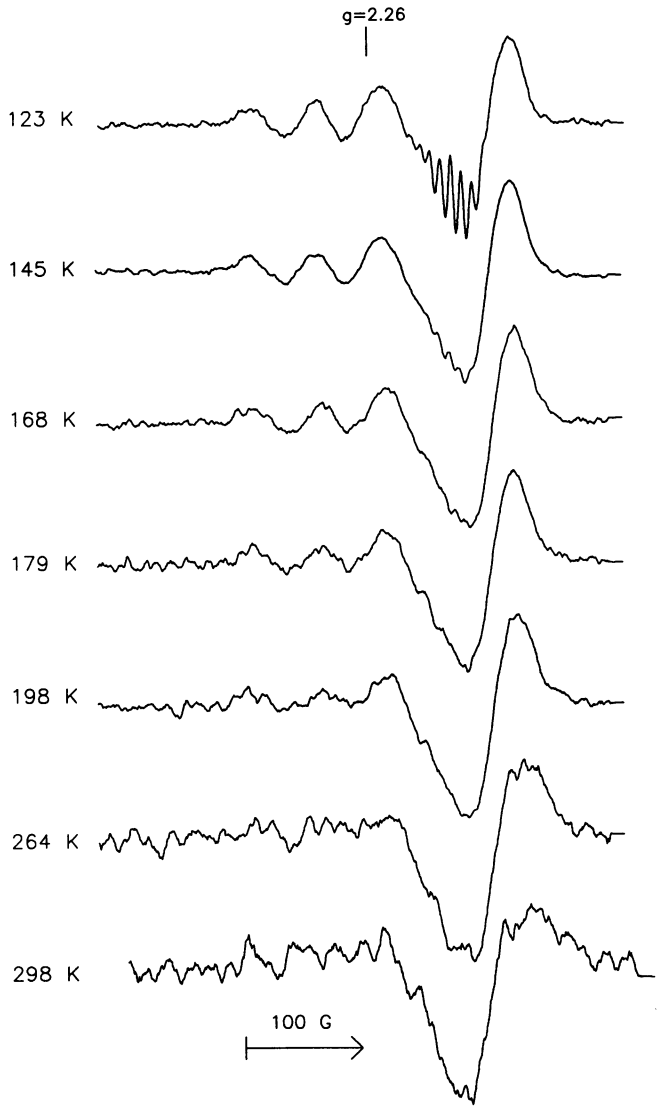

FIGURE 2 Second derivative S-band (2.35 GHz) spectra of the cupric site of azurin at 123 K, 36 scans; 198 K, 30 scans; 264 K, 25 scans; 298 K, 54 scans, etc.; scan time, 2 min; modulation frequency, 100 and 1 kHz.

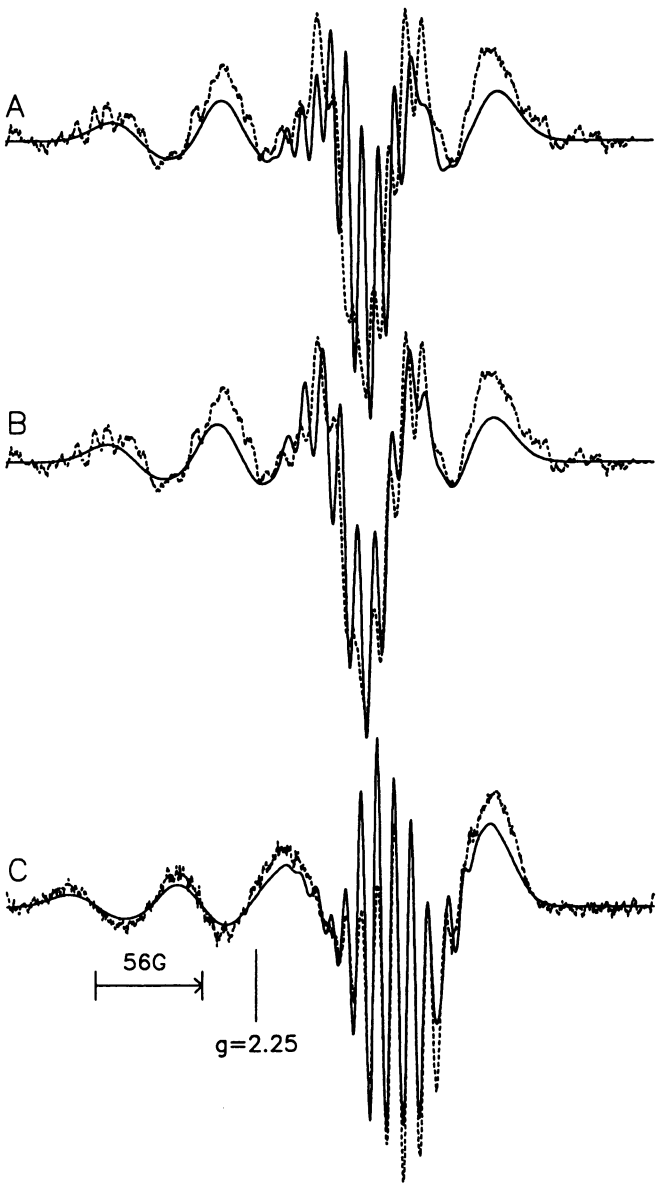

FIGURE 3 Second derivative L-band (1.64 GHz) spectra (*dashed lines, A* and *B*) at ~20 K for the cupric site from azurin. Modulation frequencies, 100 kHz and 270 Hz; time constant, 0.1 s; scan time, 1 min; microwave power set at 22 dB. The first harmonic (*dashed lines, C*) of the experimental S-band spectrum described in Fig. 4. Simulations with parameters from Table 2 except for (*A*) A_x = 46 MHz; for (*B* and *C*) A_x = 30 MHz.

ative spectrum (Fig. 2, *top spectrum*) or the first harmonic of the first derivative spectrum (Fig. 3 *C*).

The EPR spectrum from the copper site in azurin changes as the temperature increases. A decrease in the resolution of the superhyperfine structure in the $g_\perp$ region of the S-band spectrum was observed as the temperature was raised from 123 K to room temperature (Fig. 2). The resolution was much improved upon lowering the temperature from 123 to 20 K, but no additional lines were resolved (compare Fig. 2, *top spectrum,* with Fig. 3 *C*). Very little data are available for the complex $g_\perp$ region of EPR spectra, but the improved resolution at S-band and 20 K may be close to optimum with respect to ligand hyperfine structure. Although superhyperfine structure was not visible in the L-band spectrum at 120 K (Fig. 1), it was clearly resolved at 20 K (see Fig. 3).

The superhyperfine structure in the $g_\perp$ region and the Cu(II) hyperfine lines in the $g_\parallel$ region of the EPR spectra are lost as the temperature increases (Fig. 2). Bacci and Cannistraro (22) have studied the role of vibronic coupling for the temperature dependence of the *g*-strain in proteins containing a type 1 Cu(II) binding site. During the motion in the (anharmomic) potential well, excited electronic states are coupled to the ground state to variable extents, depending on the quantum of the vibration. In this case, the *g*-tensor and hyperfine values are really functions of the mean vibronic amplitude of the *n*th level. The superhyperfine structure may also be sensitive to vibronic motion and is lost as the temperature is raised.

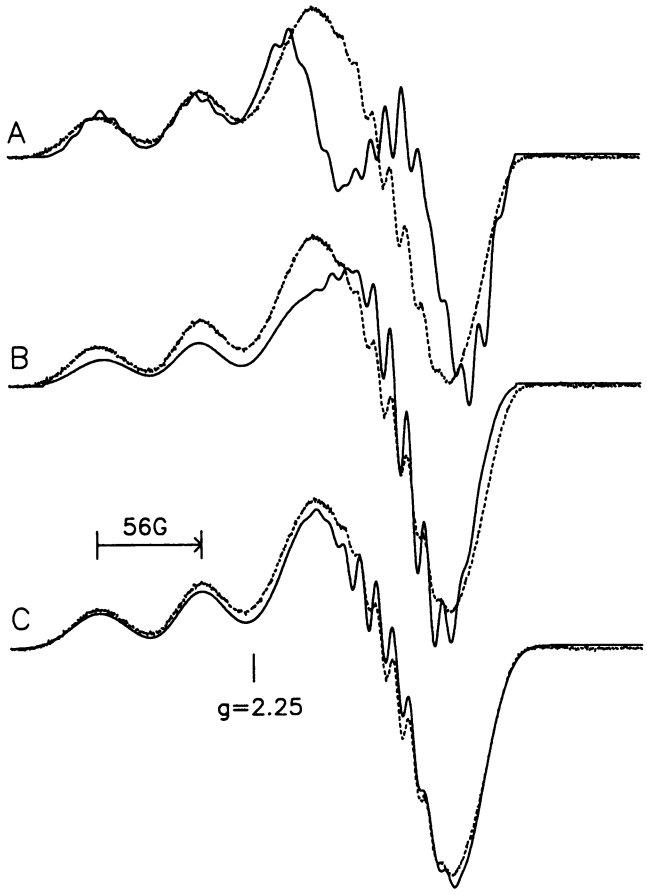

FIGURE 4 First derivative S-band (2.3 GHz) spectrum at ~20 K for the cupric site from azurin (*dashed* lines). Modulation amplitude, 1 G; modulation frequency, 100 kHz; time constant, 0.03 s; microwave power, 0.2 mW. Simulations with the parameters from Table 2 except for (*A*) $A_y = A_x$ = 66 MHz and the Euler angles are zero; for (*B*) A_y = 18 MHz and A_x = 46 MHz and the Euler angles are zero; and for (*C*) A_y = 18 MHz and A_x = 30 MHz.

TABLE 1 **Original parameters from literature (published values)*‡**

	g	A^{Cu}	A^{N1}	A^{N2}	A^{H1}	A^{H2}	P_i^{Cu}
$g_\perp$	2.052	66					
$g_\parallel$	2.263	161	27	17	23	18	5.5

* Werst et al., 1991; Roberts et al., 1984. ‡Hyperfine and quadrupole (P_i^{Cu}) terms in MHz.

From the x-ray crystal structure (3, 2) and the Q-band (35 GHz) ENDOR data (11), there is little doubt that the ligand hyperfine couplings are due to 2N from two coordinated imidazole rings (His46 and His117) and 2H from the methylene protons adjacent to the coordinated sulfur of Cys112. The relatively large electron spin densities on these protons are attributed to the high degree of covalency of the Cu-S bond with Cys112, and is supported by theoretical models (23).

In the most simple case, where the Cu(II) signal is axial (i.e., $g_x = g_y$) and the ligand hyperfine couplings are all equivalent, a 7-line superhyperfine pattern with 1:4:8:10:8:4:1 intensity would be expected for each of the four Cu hyperfine transitions in the perpendicular region, that is, 4 overlapping sets of 7 lines. The resolution in this region would therefore depend on the magnitudes of the copper and ligand hyperfine couplings and the resulting overlapping patterns. In reality, the EPR spectrum for azurin is further complicated by a slightly rhombic g-tensor (i.e., $g_x \neq g_y$ [8]), ligand hyperfine couplings which are not equivalent (11) and "overshoot" lines (or anomalous Cu lines), and possibly by lines from forbidden transitions and shifts due to quadrupole terms (7). At 20 K, at least 8–10 lines were resolved in the second derivative spectrum of the perpendicular region at both 1.16 and 2.35 GHz (Fig. 3).

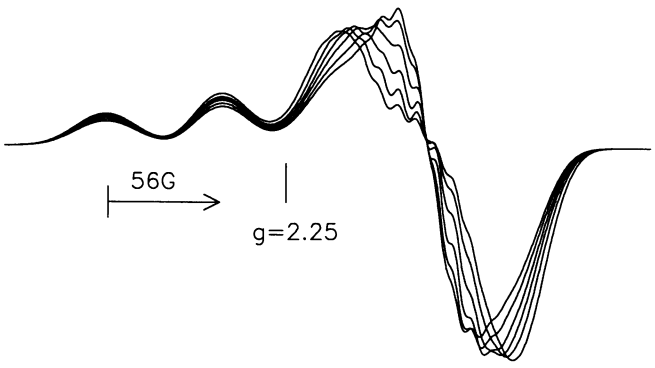

FIGURE 5 First derivative simulated S-band spectra in which the hyperfine constant for copper, A_x, is varied from 10 to 60 MHz (*left-to-right* on high field side). EPR parameters except for A_x are given in Table 2. The microwave frequency for these simulations is 2.2379 GHz.

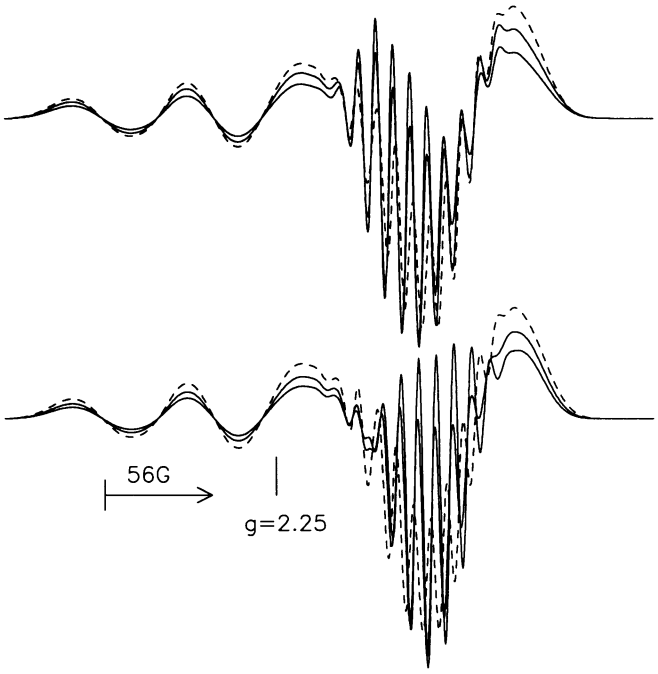

FIGURE 6 Second derivative simulated S-band spectra in which the Euler angle, α, is varied from 0 to 20 to 40° (*top spectra*) and from 40 to 60 to 80° (*bottom spectra*). The dashed lines mark the 40° spectrum in both sets. EPR parameters given in Table 2.

Simulations

Computer simulations of the EPR experimental data at 1.16 and 2.35 GHz are shown in Figs. 3 and 4. To somewhat simplify the calculations, certain assumptions were made. First, since the two strong proton couplings from

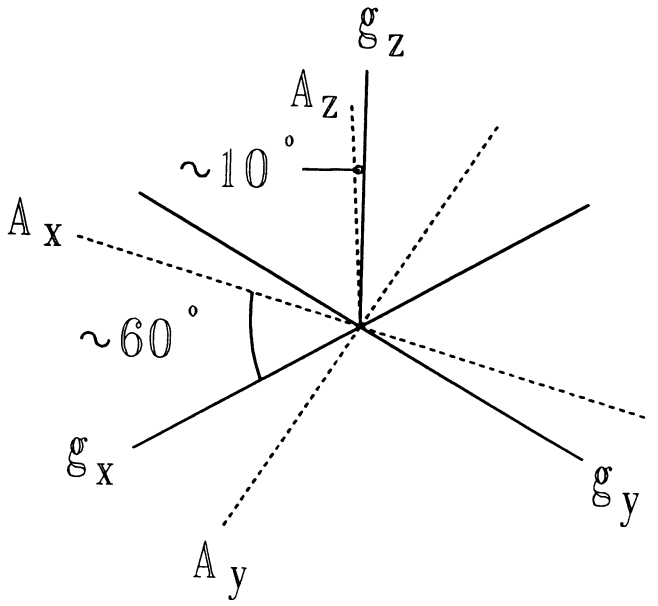

FIGURE 7 Relative axes for g- and A-tensors.

TABLE 2 **EPR parameters from simulations***

	g	A^{Cu}	Euler angles	A^{N1}	A^{N2}	A^{H}	W	A-strain	g-strain
x	2.032	30 (46)	60 (α)	27	21	24	6	−0.01	0.001
y	2.047	18	10 (β)	25.5	18	18	10	−0.5	0.1
z	2.253	172.2	10 (γ)	27	17.5	21	14	−25	6

Quadrupole parameters: QD, 5.5; QE, −1.0. *Hyperfine and quadrupole terms in MHz.

Cys112 differed by only 5 MHz (11), they were made to be equivalent at an intermediate value (Table 2). Furthermore, since both proton and both nitrogen tensors were found to be nearly isotropic, little effect from rotation of these tensors was anticipated, and the Euler angles for these tensors were not varied. Finally, higher order terms in the equations which define the hyperfine couplings were not included and may lead to small discrepancies in the relative intensities of the various transitions of the simulation (24).

Simulations to which the previously published parameters were strictly adhered (see Table 1) did not adequately describe the low frequency EPR experimental data for *P. aeruginosa* azurin. The discrepancy between the simulated and experimental data is shown in Fig. 4 *A* for the first derivative S-band spectrum. The broad doublet in the $g_\perp$ region of the simulated spectrum collapses to a single line when the copper hyperfine was reduced to ≤46 MHz (Fig. 4 *B*). Aqualino et al. (9) also set an upper limit of about 54 MHz for $A_\perp$ and simulate spectra with A_x and A_y of ~45 MHz. Fig. 5 shows more clearly the effect on the lineshape by varying A_x^{Cu} from 10 to 60 MHz in 10 MHz increments. Use of the second derivative spectra permitted more precise parameters to be extracted from the simulations through visual inspection of the fit between the simulated and experimental data, and optimum values obtained for A_x and A_y in this way were 30 and 18 MHz, respectively.

The fit of the simulated to the experimental data improved further when the Euler angles for the copper hyperfine were varied in 10° increments relative to the g-tensor (Fig. 6). An optimum value of 50–60° was determined for α, the angle of rotation of the A-tensor axis system about the z-axis (see Fig. 7). Setting α at 60° and varying the second Euler angle β (rotation about the new x-axis) caused large changes in the lineshape. A value of only 10° was determined to be optimum for β. Since β is a small angle, rotation of γ about the new z-axis was expected to vary much like rotation of α, and a value of 10° was arbitrarily selected. The final Hamiltonian parameters used to simulate the EPR data are listed in Table 2. It is important to note that the parameters in Table 2 have not been changed for simulations at X-, S- and L-band frequencies. The low symmetry of the cupric site in azurin increases the number of EPR parameters, but multifrequency data are used to determine as many EPR parameters as are sensitive to the data.

Non-coincident g- and A-tensors and a buildup of spectral intensity, i.e., an "overshoot" from the superposition of the set of all orientations having the same g-value may explain the previously reported value of 66 MHz for $A_\perp^{Cu}$ (10). It should be noted that the orientation of the trigonal plane about Cu(II) containing the approximately coplanar S(Cys112), N(His46), and N(His117) ligands has not been determined with respect to the g- and A-tensor axes. Additional studies such as ENDOR-induced EPR would be necessary to determine the angle between the Cu-N bond axis and the g_x-axis (25).

Inclusion of quadrupole terms broadened the hyperfine structure in the simulations. This broadening was offset by reducing the linewidth parameters. It appears that a minimum linewidth of the $M_I = -3/2$ and $-1/2$ lines in the $g_\parallel$ region is ~16 G (Table 3). Reducing the correlation coefficient, a measure of the degree of correlation of the g- and A-strains (12) from 1.0 to 0.5 had little effect on the linewidths and lineshape. Parameters for g- and A-strain were also added to contribute to the linewidth. Whether these linewidth and strain parameters listed in Tables 2 and 3 are unique is uncertain, but general trends are probably valid. For example, the linewidth parameters for the x- and y-axes are less than for the z-axis. This is consistent with small changes in the Euler angles and/or strains. Strains involving the Euler angles β and γ result in large changes in linewidths because of the relatively large anisotropy in the xz or yz planes. Small absolute values of the parameters and/or less anisotropy give sharper lines in the xy plane. Although significant resolution of ligand hyperfine in the $g_\perp$ region of the type 1 copper site in azurin has been obtained, additional methods such as multiquantum EPR (26) may be required to improve the resolution of the fine structure in the $g_\parallel$ region.

Aqualino et al. (9) have obtained frozen-solution EPR spectra at 6, 9, and 35 GHz. Anomalies in the splitting

TABLE 3 **Linewidths in $g_\parallel$ region***

Frequency	Temperature	$M_I = -3/2$	$M_I = -1/2$
X	22 K	21	~25
S	~120 K	18	18
S	20 K	18	16
L	~120 K	17	18

* Halfwidth at half height in Gauss.

and shapes of the lines in the $g_{||}$ region are simulated assuming a correlated distribution in spin-Hamiltonian parameters. Because the $M_I = +1/2$ line in the $g_{||}$ region at low frequencies was obscured by the intense features in the $g_\perp$ region, anomalies in the splittings of the lines were not detected. But even though only the $M_I = -3/2$ and $-1/2$ lines are resolved at low frequencies, large values for the strain parameters for the $g_{||}$ lines (Table 2) were used to simulate the $g_{||}$ lines in the S-band spectrum (Figs. 3 *C* and 4 *C*). At low frequencies, strain is minimized and may not be as dominant a factor as at 6, 9, and especially 35 GHz (9). Thus, the effect of non-coincidence of the *g*- and *A*-tensors on spectral shape at low frequencies (Fig. 6) is substantial, whereas a small change in hyperfine separation with non-coinciding principal axes of the *g*- and *A*-tensors does not explain the collapse of hyperfine structure at 35 GHz (9).

In summary, we have used the low temperature EPR spectra at various frequencies to refine the Hamiltonian parameters which describe the Cu(II) site in *P. aeruginosa* azurin, particularly in the complex $g_\perp$ region of the spectrum. Parameters have been found that yield a simulated spectrum, consistent with the experimental one. We cannot exclude the possibility that other choices of parameters may do as well; however, the fact that the same parameters can be used to fit spectra at different microwave frequencies is extremely encouraging.

Initial attempts by M. Pasenkiewicz-Gierula to simulate the multifrequency data, transfer of the simulation program to our computer by J. Ratke, S-band data at 20 K from M. Newton, and simulations from J. Ratke are greatly appreciated.

This work was supported by the National Science Foundation grant No. DMB 9105519 (to W. Antholine) and National Institutes of Health grants RR-01008 and GM-22764 (to D. McMillin).

Received for publication 29 June 1992 and in final form 30 September 1992.

REFERENCES

1. Adman, E. T. 1991. Copper protein structures. *Adv. Prot. Chem.* 42:145–197.
2. Nar, H., A. Messerschmidt, R. Huber, M. van de Kamp, and G. W. Canters. 1991. X-ray crystal structure of the two site-specific mutants His35Gln and His35Leu of azurin from *Pseudomonas aeruginosa*. *J. Mol. Biol.* 218:427–447.
3. Adman, E. T., R. E. Stenkamp, L. C. Sieker, and L. H. Jensen. 1978. A crystallographic model for azurin at 3 Å resolution. *J. Mol. Biol.* 123:35–47.
4. Baker, F. N. 1988. Structure of azurin from *Alcaligene denitrificans*. *J. Mol. Biol.* 203:1071–1095.
5. McMillin, D. R., R. C. Rosenberg, and H. B. Gray. 1974. Preparation and spectroscopic studies of cobalt(II) derivatives of blue copper proteins. *Proc. Natl. Acad. Sci. USA.* 71:4760–4762.
6. Tennent, D. L., and D. R. McMillin. 1979. A detailed analysis of the charge-transfer bands of a blue copper protein. Studies of the nickel(II), manganese(II), and cobalt(II) derivatives of azurin. *J. Am. Chem. Soc.* 101:2307–2311.
7. Vänngård, T. 1972. Copper proteins. *In* Biological Applications of Electron Spin Resonance. H. M. Swartz, J. R. Bolton, and D. C. Borg, editors. Wiley-Interscience, New York. 411–447.
8. Groeneveld, C. M., R. Aasa, B. Reinhammar, and G. W. Canters. 1987. EPR of azurin from *Pseudomonas aeruginosa* and *Alcaligenes denitrificans* demonstrates pH-dependence of the copper site in *Pseudomonas aeruginosa* protein. *J. Inorg. Biochem.* 31:143–154.
9. Aqualino, A., Brill, A. S., Bryce, G. F., and Gerstman, B. S. 1991. Correlated distributions in *g* and *A* tensors at a biologically active low-symmetry cupric site. *Phys. Rev. A* 44:5257–5271.
10. Roberts, J. E., J. F. Cline, V. Lum, H. Freeman, H. B. Gray, J. Peisach, B. Reinhammar, and B. M. Hoffman. 1984. Comparative ENDOR study of six blue copper proteins. *J. Am. Chem. Soc.* 106:5324–5330.
11. Werst, M. M., C. E. Davoust, and B. M. Hoffman. 1991. Ligand spin densities in blue copper proteins by Q-band ^{1}H and ^{14}N ENDOR spectroscopy. *J. Am. Chem. Soc.* 113:1533–1538.
12. Froncisz, W., and J. S. Hyde. 1980. Broadening by strains of lines in the *g*-parallel region of Cu^{2+} EPR spectra. *J. Chem. Phys.* 73:3123–3131.
13. Sealy, R. C., J. S. Hyde, and W. E. Antholine. 1985. Electron spin resonance. *In* Modern Physical Methods in Biochemistry. A. Neuberger and L. L. M. VanDeenen, editors. Elsevier, Amsterdam. 109–129.
14. Hanna, P. M., D. R. McMillin, M. Pasenkiewicz-Gierula, W. E. Antholine, and B. Reinhammar. 1988. Type 2-depleted fungal laccase. *Biochem. J.* 253:561–568.
15. Ambler, R. P., and L. H. Brown. 1967. The amino acid sequence of *Pseudomonas fluorescens* azurin. *Biochem. J.* 104:784–825.
16. Hutnick, C. M., and A. G. Szabo. 1989. Confirmation that multiexponential fluorescence decay behavior of holoazurin originates from conformational heterogeneity. *Biochemistry.* 28:3923–2934.
17. Blaszak, J. A., D. R. McMillin, A. T. Thorton, and D. L. Tennent. 1983. Kinetics of copper(II) uptake by apoazurin in complexing media. *J. Biol. Chem.* 258:9886–9892.
18. Froncisz, W., and J. S. Hyde. 1982. The loop gap resonator: a new microwave lumped circuit ESR sample structure. *J. Magn. Res.* 47:515–521.
19. Hyde, J. S., A. Jesmanowicz, J. J. Ratke, and W. E. Antholine. 1992. Pseudomodulation: a computer based strategy for resolution enhancement. *J. Magn. Res.* 96:1–13.
20. Nilges, M. J. 1979. Electron Paramagnetic Resonance Studies of Low Symmetry Nickel(I) and Molybdenum(V) Complexes. Ph.D. dissertation, University of Illinois, Urbana, IL.
21. Maurice, A. M. 1980. Acquisition of Anisotropic Information by Computational Analysis of Isotropic EPR Spectra. Ph.D. dissertation, University of Illinois, Urbana, IL.
22. Bacci, M., and S. Cannistraro. 1990. Role of vibronic coupling and of conformational substrate distribution in determining features of copper-protein EPR spectra. *Appl. Magn. Res.* 1:369–378.
23. Penfield, K. W., A. A. Gewirth, and E. I. Solomon. 1985. Electronic structure and bonding of the blue copper site in plastocyanin. *J. Am. Chem. Soc.* 107:4519–4529.
24. Pilbrow, J. 1990. Transition Ion Electron Paramagnetic Resonance. Clarendon Press, Oxford. 243–259.
25. Greiner, S. P., R. W. Kreilick, and K. A. Kraft. 1992. Angle selection in EPR and ENDOR spectra of rhombic metal complexes: copper glutamate and copper [^{15}N] glutamate spectra. *J. Am. Chem. Soc.* 114:391–399.
26. Sczaniecki, P. B., and J. S. Hyde. 1991. Continuous wave multiquantum electron paramagnetic resonance spectroscopy. II. Spin-system generated intermodulation sidebands. *J. Chem. Phys.* 94:5907–5916.